

# Effect of AlGa<sub>N</sub> interlayer on luminous efficiency and reliability of GaN-based green LEDs on silicon substrate\*

Jiao-Xin Guo(郭娇欣), Jie Ding(丁杰)<sup>†</sup>, Chun-Lan Mo(莫春兰), Chang-Da Zheng(郑畅达),  
Shuan Pan(潘拴), and Feng-Yi Jiang(江风益)

National Institute of LED on Silicon Substrate, Nanchang University, Nanchang 330096, China

(Received 16 November 2019; revised manuscript received 11 January 2020; accepted manuscript online 24 February 2020)

The effect of AlGa<sub>N</sub> interlayer in quantum barrier on the electroluminescence characteristics of GaN-based green light emitting diodes (LEDs) grown on silicon substrate was investigated. The results show that AlGa<sub>N</sub> interlayer is beneficial to improve the luminous efficiency of LED devices and restrain the phase separation of InGa<sub>N</sub>. The former is ascribed to the inserted AlGa<sub>N</sub> layers can play a key role in determining the carrier distribution and screening dislocations in the active region, and the latter is attributed to the increased compressive stress in the quantum well. However, when the electrical stress aging tests were performed at a current density of 100 A/cm<sup>2</sup>, LED devices with AlGa<sub>N</sub> interlayers are more likely to induce the generation/proliferation of defects in the active region under the effect of electrical stress, resulting in the reduced light output power at low current density.

**Keywords:** green LED, AlGa<sub>N</sub> interlayer, external quantum efficiency, reliability

**PACS:** 73.61.Ey, 85.60.Jb, 73.21.Fg, 78.60.Fi

**DOI:** 10.1088/1674-1056/ab7903

## 1. Introduction

In recent years, although the external quantum efficiency (EQE) of GaN-based green light-emitting diodes (LEDs) has been improved rapidly. However, there are still two problems that need to be solved urgently, one is the efficiency droop,<sup>[1,2]</sup> and the other is the degradation of the light output power.<sup>[3]</sup> Aiming at the problem of efficiency droop, several possible mechanisms have been proposed, such as electron leakages,<sup>[4]</sup> carrier delocalization,<sup>[5]</sup> insufficient carrier injection efficiency,<sup>[6]</sup> and Auger recombination.<sup>[7]</sup> However, these mechanisms are still controversial, and the precise physical mechanisms that cause efficiency droop are still remained obscure until now. In addition, some researchers have studied the carrier distribution in the active region and its influence on the efficiency droop, and reported that the carrier distribution is a key factor affecting both the peak efficiency and efficiency droop.<sup>[8]</sup> To obtain high-efficiency GaN-based LEDs, many works have been carried out in optimizing GaN-based LEDs structures, and the use of AlGa<sub>N</sub> layers in GaN-based LEDs structures is a practical design method. Lin *et al.*<sup>[9]</sup> reported that the inserted AlGa<sub>N</sub> layer between the n-type GaN layer and the InGa<sub>N</sub> active region can obtain higher peak efficiency and reduce efficiency droop at higher injection level. Wu *et al.*<sup>[10]</sup> showed that the unintentionally doped electron barrier layer (EBL) grown at low temperature could increase the proportion of hole current in V-shape pits (V-pits). Recently, Wang *et al.*<sup>[11]</sup> found that the inserted AlGa<sub>N</sub> interlayers in the four quantum barriers near the n-layer can regulate

the carrier distribution and improve the luminous efficiency.

Meanwhile, the reliability and lifetime issues of GaN-based LEDs are becoming increasingly prominent. There are many factors that affect the reliability of GaN-based LEDs. It is generally believed that the degradation of GaN-based LED devices is the result of various mechanisms. Several explanations for device degradation have been proposed, including non-radiative recombination centers generated in the active region,<sup>[12–14]</sup> changes in the carrier injection mechanism,<sup>[15]</sup> degradation of packaging materials,<sup>[16]</sup> degradation of Ohmic contact,<sup>[17]</sup> and electromigration of metals.<sup>[18]</sup> However, most of these works focused on the failure mechanism of GaN-based LED devices in the stressing process, and paid little attention to the effect of epitaxial structure changes on the reliability of GaN-based LED devices. To obtain the GaN-based LED devices with high efficiency and high reliability, it is necessary to verify the reliability of the optimized GaN-based LED.

In this paper, AlGa<sub>N</sub> interlayer was inserted in the quantum barrier of the GaN-based green LED grown on silicon substrates to investigate its effect on the luminous efficiency and the reliability of LED devices under the electrical stress.

## 2. Experiments

Two samples were grown on patterned 2-inch (1 inch = 2.54 cm) Si(111) substrates by metal-organic chemical vapor deposition (MOCVD) system. As illustrated in Fig. 1, epitaxy started from an AlN buffer layer, then a Si-doped n-GaN

\*Project supported by the National Key Research and Development Program of China (Grant Nos. 2016YFB0400600 and 2016YFB0400601) and the National Natural Science Foundation of China (Grant Nos. 61704069 and 51705230).

<sup>†</sup>Corresponding author. E-mail: [ncudj@163.com](mailto:ncudj@163.com)

layer was grown on the AlN buffer. Subsequently, 32 periods of InGaN/GaN superlattices layers (SLs) were deposited on the n-GaN layer. Then followed by a low temperature-GaN layer. After that, 10 periods of InGaN/GaN multi-quantum wells (MQWs) were grown. The thickness of each quantum well is fixed at 28 Å and the thickness of quantum barrier is variable. The quantum barriers from n-GaN to p-GaN are divided to three types with 130-Å quantum barrier, 100-Å quantum barrier and 90-Å quantum barrier respectively, so as to enhance holes injection into the MQWs by tunneling process.<sup>[19]</sup> The difference of samples A and B is only in the MQW structure which is marked as green region 1 and green region 2. For sample A, the four quantum barriers near the n-layer (green region 1) are 130-Å-thick GaN and the last quantum barrier (green region 2) is 90-Å-thick GaN. For sample B, the four quantum barriers near the n-layer (green region 1) consist of 50-Å-GaN/55-Å-Al<sub>0.1</sub>Ga<sub>0.9</sub>N/25-Å-GaN and the last quantum barrier (green region 2) is 50-Å-Al<sub>0.1</sub>Ga<sub>0.9</sub>N/40-Å-

GaN. A p-layer was grown successively after the MQWs and it consists of p-AlGaN EBL, heavily Mg-doped p-GaN layer, p-AlGaN/InGaN superlattice layer, lightly Mg-doped p-GaN layer, and heavily Mg-doped p-GaN contact layer. The as-grown epitaxial wafers then were fabricated into vertical thin film LEDs chip in size of 1 mm × 1 mm. Then, the LED chips with dominant wavelength of 520 nm (at current density of 35 A/cm<sup>2</sup>) were selected and packaged in an LUXEON structure. In order to avoid the influence of the encapsulating material during the stress stage, no encapsulating material was applied on the chips of both samples. A group of ten LEDs were selected from each sample and stressed under forward current density of 100 A/cm<sup>2</sup> in an isothermal chamber (40 °C) for up to 1000 hours. The electroluminescence properties of the LEDs before and after stress were tested under continuous wave mode by Keithley Instruments 2635A source meter and Instrument Systems CAS 140CT spectrometer.

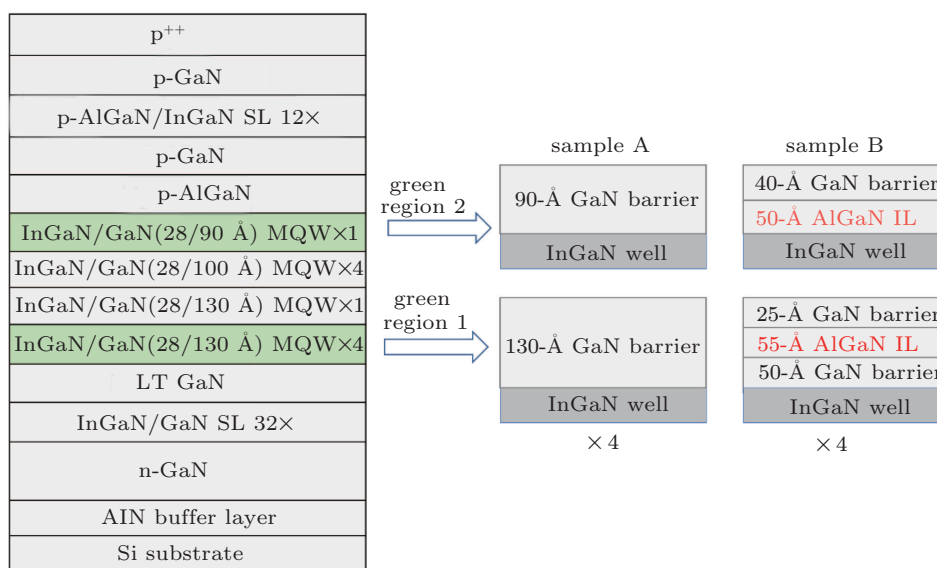


Fig. 1. Schematic epitaxial structure of the experimental samples A and B.

### 3. Results and discussion

Figures 2(a) and 2(b) show the curves of EQE as functions of current density and the voltage–current curves of two samples before stress, respectively. As shown in Fig. 2(a), sample B with AlGaN interlayer in the quantum barriers has significantly higher luminous efficiency than sample A, especially at low current, and lower leakage current as shown in Fig. 2(b). The reason is attributed to the insertion of the AlGaN interlayers in the quantum barriers, which can effectively improve the role of V-pits in screening dislocations and regulate the distribution of carriers.<sup>[11]</sup> Due to the AlGaN interlayer in the last barrier of sample B, more proportion of holes will be injected from the sidewall of the V-pits into the *c*-plane quantum wells to participate in radiative recom-

ination, and the carrier's distribution in the quantum wells is more uniform.<sup>[20,21]</sup> The AlGaN interlayers in the quantum barriers of sample B has higher energy barrier than GaN barrier, thereby increasing the effect of V-pits on screening dislocations and reducing defect-related non-radiative recombination, which also corresponds to the lower leakage current.<sup>[11]</sup> Therefore, the luminous efficiency at low current density is significantly improved due to the AlGaN interlayers.

Figures 2(c) and 2(d) show peak wavelength and full width at half maximum (FWHM) as functions of current density for the two samples before stress. In comparison with sample A, the sample B has longer peak wavelength at low current density and shorter peak wavelength at high current density as shown in Fig. 2(c). The FWHM of sample B is wider than sample A over the entire test current density range

as shown in Fig. 2(d). Due to the obstruction of high energy barrier of AlGa<sub>N</sub> interlayers in the quantum barriers, a larger proportion of carriers participate in radiative recombination in the quantum wells near the p-layer at low current for sample B. Compared with sample A, the insertion of AlGa<sub>N</sub> interlayers in the quantum barriers of sample B will bring greater compressive stress to the quantum wells,<sup>[22]</sup> and less carriers in the quantum wells near the n-layer, leading to weakening of the screening polarized electric fields, so that the quantum-confined Stark effect (QCSE) becomes stronger. Therefore, the energy band becomes more tilted and the band gap narrows, resulting in longer emission wavelength and wider FWHM. As the current density increases, the quantum wells near the p-layer have been filled with carriers, and the number of carriers participating in radiative recombination in the quantum wells near the n-layer increases. Sample B consumes more carriers to screen the polarized electric fields compared to sample A, so the peak wavelength is slightly shorter than sample A at high current density. At high current density,

the FWHM of sample A is narrower due to more quantum wells filled with carriers. Compared to sample A, sample B has two sets of emission peaks from the quantum wells near the n-layer and the p-layer, respectively, so its FWHM is still wider than sample A at high current density.

The fluorescent luminescence (FL) images of epitaxial wafers of the two samples are shown in Fig. 3. It can be clearly observed from the FL images that there are many dark spots in sample A, and the number and size of dark spots are remarkably less for sample B with AlGa<sub>N</sub> interlayers. It is generally believed that the dark spots observed from FL originate from In-rich clusters.<sup>[23]</sup> This indicates that the insertion of AlGa<sub>N</sub> interlayers in the quantum barriers is beneficial to suppress the phase separation of InGa<sub>N</sub>. The suppression is attributed to the increase of compressive stress in the quantum wells and an improvement of uniformity of In components distribution in the quantum wells for sample B with AlGa<sub>N</sub> interlayers in the quantum barriers.<sup>[24,25]</sup>

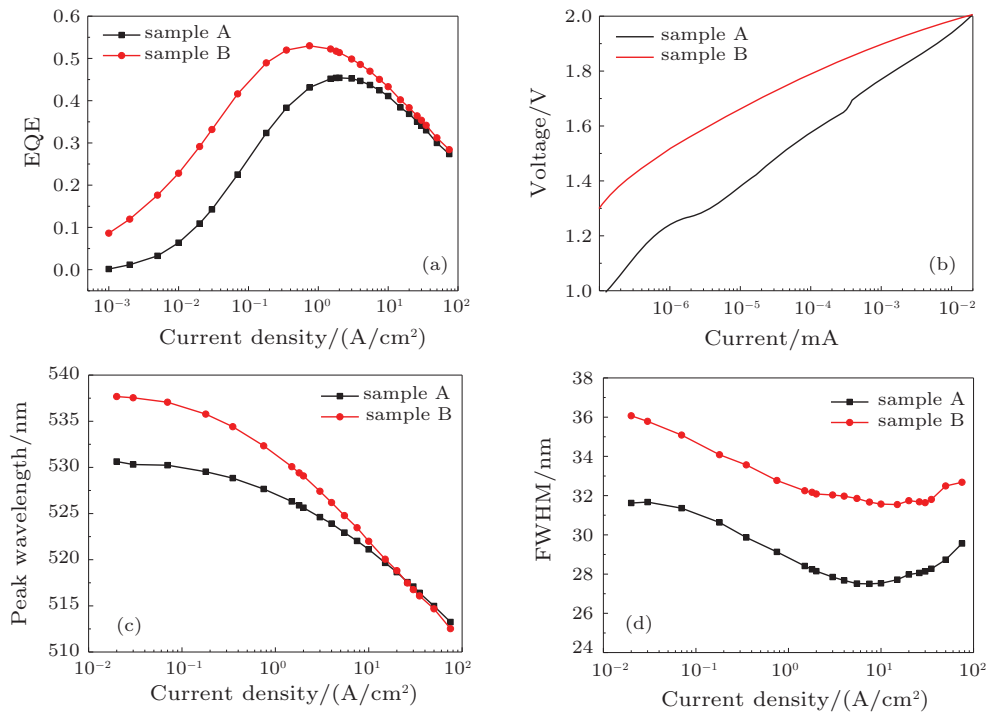


Fig. 2. (a) Plots of EQE as functions of current density for the samples. (b) *I*–*V* curves. (c) Peak wavelength as functions of current density for the samples. (d) FWHM as functions of current density for the samples.

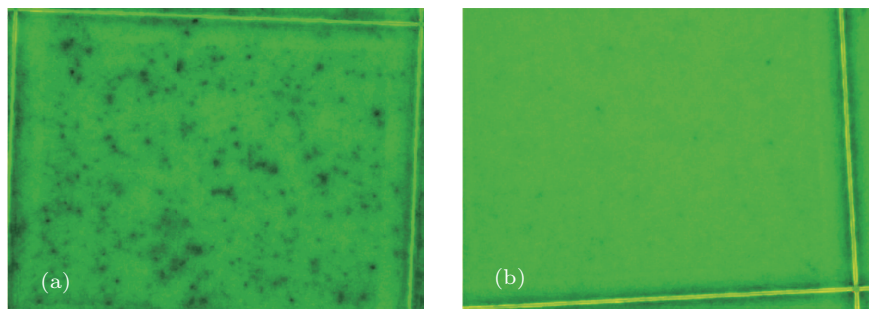


Fig. 3. FL images of epitaxial wafer of (a) sample A, (b) sample B.

The electrical stress aging tests were performed at a current density of  $100 \text{ A/cm}^2$  for both samples A and B. Figure 4 shows the normalized optical power of the two samples plotted against stress time. The optical power is measured at an injection current of  $35 \text{ A/cm}^2$ . To reduce error, the average value of each group of stressed samples are taken as the basis for consideration. It can be seen that the change of the optical power of the two samples has opposite trend with stress time. Sample A shows increased light output after stress for 1000 h, and its optical power increases by 1.32%. However, the optical power of sample B decreases monotonously with stress time, and its optical power decreases by 3.68% after stress for 1000 h. Except for the difference in epitaxial structure, the chip fabrication and packaging process of the two samples are the same. Therefore, it is preliminarily considered that the difference of light output decay between the two samples studied in this article may be due to the change of the epitaxial structure. This suggests that the insertion of AlGaIn interlayer has a negative impact on the reliability of LED devices.

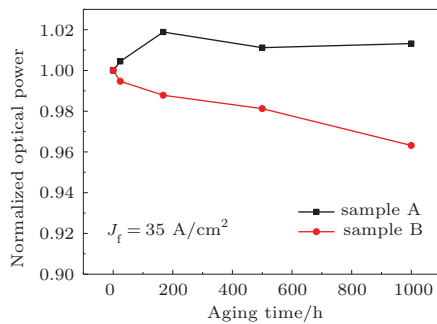


Fig. 4. Normalized optical power of samples A (black) and B (red) as a function of time.

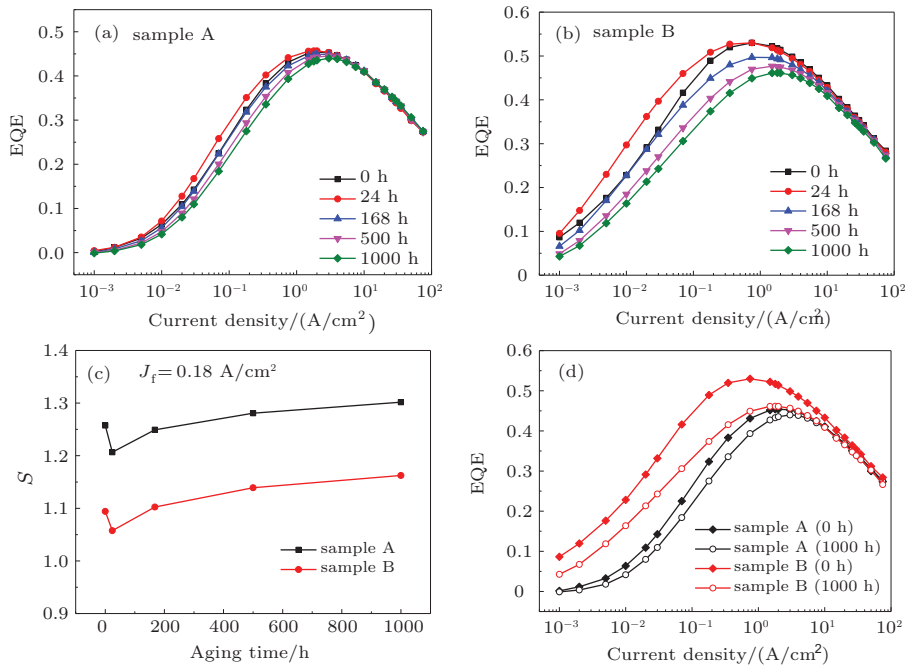


Fig. 5. EQE curves for different stress time of (a) sample A and (b) sample B. (c) Curves of  $S$  coefficient as functions of stress time of the two samples at current density of  $0.18 \text{ A/cm}^2$ . (d) Curves of EQE as functions of current density before and after 1000-h stress of the two samples.

Figures 5(a) and 5(b) are plots of EQE as functions of current density for samples A and B at different stress time points, respectively. It can be seen that the EQE of the two samples after stress for 24 h are higher than the EQE before stress at low current density, in other words, the EQE increases at low current density at the early stage of stress. With the increase of stress time, the EQE of the two samples begins to decline at low current density. The changes of EQE at high current density with stress time are not obvious which is due to the non-radiative recombination centers saturated at high current density.<sup>[26]</sup>

The increase of EQE at low current density may be due to annealing effect at the early stage of stress, which leads to an increase in luminous efficiency.<sup>[27,28]</sup> Figure 5(c) shows the  $S$  coefficient of the two samples at current density of  $0.18 \text{ A/cm}^2$  as a function of the stress time. Generally for GaN-based LEDs, the recombination mechanism of carriers can be inferred from the value of the  $S$  coefficient in the relation  $L \propto I^S$ . The  $S$  value is close to 2 when the Shockley–Read–Hall (SRH) recombination is dominant; the  $S$  value is close to 1 when the radiative recombination is dominant; and when the  $S$  value is less than 1, the carriers overflow the quantum well.<sup>[29]</sup> We can observe that the  $S$  values of the two samples initially decrease and then increase, and the  $S$  values are between the values 1 and 2. The  $S$  value of the two samples decreases at the early stress stage, and is closer to 1 after stress, indicating that the electric stress under high injection density at the early stress stage can reduce the density of SRH non-radiative recombination centers, thus the EQE increases at low current density in the early stage.

With the increase of stress time, the EQE of the two samples begins to decline at low current density, and the value of  $S$  gradually increases and is close to 2, which indicates that the non-radiative recombination increases with increasing stress time. Some studies have shown that the electric stress even at very low level could induce defects generation in the active region and then reduce luminous efficiency.<sup>[27,30]</sup> Therefore, during the stress process, the defects accumulate gradually in the active region, and the non-radiative recombination increases gradually. The EQE of sample B decreases more significantly than sample A at low current density after stress for 1000 hours as shown in Fig. 5(d), which indicates that the sample B is more likely to induce defect's generation during stressing. It is attributed to the large amounts of heat generated in the p-n junction under the combined action of electrical stress and thermal stress during the stressing process. In higher temperature environment, carriers interact with the lattice during motion, which is easy to induce generation of defects in the active region, thus increasing the probability of non-radiative recombination.<sup>[26,31]</sup> For sample B, a bigger carrier concentration in the quantum wells near the p-layer may be due to the higher energy barrier of AlGaIn interlayer, so a bigger proportion of carriers participates in the emission in the quantum wells near the p-layer thus enhancing carriers to interact with the lattice during motion, which is easy to induce the generation/proliferation of defects.<sup>[26]</sup> Secondly, because the AlGaIn interlayers are inserted in the quantum barriers, the quantum wells of sample B are subject to greater compressive stress compared with sample A, and the lattice generally releases stress by dislocation.<sup>[32]</sup> Thus, the LEDs with AlGaIn interlayers may generate some interface dislocations, which would generate defect-related deep energy levels. The change in the FWHM of the two samples during the stress process can prove this view from other side. As shown in Figs. 6(a) and 6(b), it can be seen that the FWHM of sample B is gradually increased during the stressing process, and the FWHM of sample A does not change obviously with increasing stress time. That is to say, the sample B also generates deep level defects during the stressing process, resulting in the FWHM becoming wider as the stress time increasing. Under the combined action of electrical stress and thermal stress in the stress process, hot carriers can interact with the lattice, inducing the generation/proliferation of defects in the active region.<sup>[26,31]</sup> The superposition of the above two factors causes the sample B to accumulate more defects during the stressing process, and increases the non-radiative recombination rate, so the EQE of sample B decreases more greatly at low current density. Although sample B generates more defects during stressing, some defect-related non-radiative recombination is shielded

due to the role of AlGaIn higher energy barrier. Therefore, even if the sample B is more prone to cause the generation or proliferation of defects during stressing, its luminous efficiency is still higher than sample A.

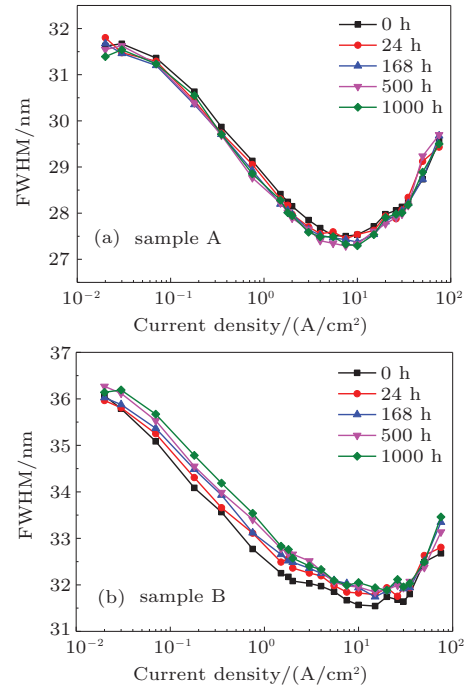


Fig. 6. FWHM as functions of current density during stressing (a) sample A, (b) sample B.

#### 4. Conclusions

In conclusion, the AlGaIn interlayers in the quantum barriers can effectively improve the role of V-pits in screening dislocations and regulate the carrier distribution, thereby greatly improving the luminous efficiency of LED devices. However, the insertion of AlGaIn interlayers could more easily induce the generation or proliferation of defects in the active region of the device during stress, which leads to a large light decay of the LED devices at low current density. Due to the regulative effect of AlGaIn on the distribution of carriers, a large proportion of carriers participates in the emission of quantum wells near the p-layer, which makes the hot carriers more likely to interact with the lattice under stress, and thus easily induce the generation or proliferation of defects. In addition, the quantum wells are subject to greater compressive stress due to AlGaIn interlayers inserted in the quantum barriers, thus alleviating the phase separation of InGaIn. However, it may cause some interface dislocations, which tends to induce the generation or proliferation of defects in the active region during stress. Therefore, it is debatable that should we insert AlGaIn interlayer into the quantum barriers to improve the optoelectronic performance of LED devices or not? In fact, the inserted AlGaIn interlayers can enhance the luminous properties but may

also reduce the reliability of LED. How to find a way to balance the luminous properties and reliability still needs further research work.

## References

- [1] Tong J H, Zhao B J, Ren Z W, Wang X F, Chen X and Li S T 2013 *Chin. Phys. Lett.* **30** 058503
- [2] Zhao Y K, Li Y F, Huang Y P, Wang H, Su X L, Ding W and Yun F 2015 *Chin. Phys. B* **24** 056806
- [3] Lin Y, Zhang Y, Guo Z Q, Zhang J H, Huang W L, Lu Y J, Deng Z H, Liu Z G and Cao Y G 2015 *Opt. Express* **23** 979
- [4] Vampola K J, Iza M, Keller S, Denbaars S P and Nakamura S 2009 *Appl. Phys. Lett.* **94** 061116
- [5] Wang J X, Wang L, Zhao W, Hao Z B and Luo Y 2010 *Appl. Phys. Lett.* **97** 201112
- [6] Zhao H P, Liu G Y, Arif R A and Tansu N 2010 *Solid State Electron.* **54** 1119
- [7] Justin I, Lucio M, Jacques P, Speck J S and Claude W 2013 *Phys. Rev. Lett.* **110** 177406
- [8] Fu J, Zhao L, Ning Z, Wang J and Li J 2015 *Journal of Solid State Lighting* **2** 5
- [9] Lin R M, Lai M J, Chang L B and Huang C H 2010 *Appl. Phys. Lett.* **97** 181108
- [10] Wu X M, Liu J L, Quan Z J, Xiong C B, Zheng C D, Zhang J L, Mao Q H and Jiang F Y 2014 *Appl. Phys. Lett.* **104** 221101
- [11] Wang Z X, Mo C L, Zheng C D, Wu X M, Liu J L and Jiang F Y 2019 *Superlattices Microstruct.* **128** 307
- [12] Meneghini M, Lago M D, Rodighiero L, Trivellin N, Zanoni E and Meneghesso G 2012 *Microelectron. Reliab.* **52** 1621
- [13] La Grassa M, Meneghini M, De Santi C, Mandurrino M, Goano M, Bertazzi F, Zeisel R, Galler B, Meneghesso G and Zanoni E 2015 *Microelectron. Reliab.* **55** 1775
- [14] Zhang N, Wei X C, Lu K Y, Feng L S, Yang J, Xue B, Liu Z, Li J M and Wang J X 2016 *Chin. Phys. Lett.* **33** 117302
- [15] Zhang T R, Fang F, Wang X L, Zhang J L, Wu X M, Pan S, Liu J L and Jiang F Y 2019 *Chin. Phys. B* **28** 067305
- [16] Fu J J, Zhao L X, Cao H C, Sun X J, Sun B J, Wang J X and Li J M 2016 *AIP Adv.* **6** 055219
- [17] Meneghini M, Rigutti L, Trevisanello L R, Cavallini A, Meneghesso G and Zanoni E 2008 *J. Appl. Phys.* **103** 063703
- [18] Kim H, Yang H, Huh C, Kim S W, Park S J and Hwang H 2000 *Electron. Lett.* **36** 908
- [19] Yoo Y S, Na J H, Son S J and Cho Y H 2016 *Sci. Rep.* **6** 1
- [20] Quan Z J, Wang L, Zheng C D, Liu J L and Jiang F Y 2014 *J. Appl. Phys.* **116** 183107
- [21] Li C K, Wu C K, Hsu C C, Lu L S, Li H, Lu T C and Wu Y R 2016 *AIP Adv.* **6** 055208
- [22] Shioda T, Yoshida H, Tachibana K, Sugiyama N and Nunoue S 2012 *Phys. Status Solidi* **209** 473
- [23] Tao X X, Liu J L, Zhang J L, Mo C L, Xu L Q, Ding J, Wang G X, Wang X L, Wu X M, Quan Z J, Pan S, Fang F and Jiang F Y 2018 *Opt. Mater. Express* **8** 1221
- [24] Karpov S Y 1998 *Mrs Internet J. Nitride Semicond. Res.* **3** 16
- [25] Tabata A, Teles L K, Scolfaro L M R, Leite J R, Kharchenko A, Frey T, As D J, Schikora D, Lischka K and Furthmüller J 2002 *Appl. Phys. Lett.* **80** 769
- [26] Meneghini M, Tazzoli A, Mura G, Meneghesso G and Zanoni E 2009 *IEEE Trans. Electron Dev.* **57** 108
- [27] Liu L L, Ling M J, Yang J F, Wang X Q, Jia W and Gang W 2012 *J. Appl. Phys.* **111** 093110
- [28] Chen T T, Wang C P, Fu H K, Chou P T and Ying S P 2014 *Opt. Express* **22** A1328
- [29] Kim K S, Han D P, Kim H S and Shim J I 2014 *Appl. Phys. Lett.* **104** 091110
- [30] Manyakhin F, Kovalev A and Yunovich A E 1998 *Mrs Internet J. Nitride Semicond. Res.* **3** 53
- [31] Cao X A, Sandvik P M, Leboeuf S F and Arthur S D 2003 *Microelectron. Reliab.* **43** 1987
- [32] Lin Y S, Ma K J, Hsu C, Feng S W, Cheng Y C, Liao C C, Yang C C, Chou C C, Lee C M and Chyi J I 2000 *Appl. Phys. Lett.* **77** 2988